Inorg. Chem. **2008**, *47*, 11734−11737

A Mixed-Valence Octanuclear Iron−Oxo Pyrazolate: Assessment of Electronic Delocalization by Structural and Spectroscopic Analysis

Indranil Chakraborty,[†] Peter Baran,[†,‡] Yiannis Sanakis,[§] Athanassios Simopoulos,[§] Esteban Fachini,[†] and Raphael G. Raptis*[,†]

Department of Chemistry and the Institute of Functional Nanomaterials, University of Puerto Rico, San Juan, PR 00931-3346, Institute of Materials Science, NCSR "Demokritos", 15310 Aghia Paraskevi, Athens, Greece

Received August 2, 2008

A formally $Fe^{III}_7Fe^{II}$ complex, containing an inner Fe_4O_4-cubane and four peripheral Fe centers, is derived from the one-electron reduction of its Fe^{III}_8 precursor. Spectroscopic analysis of the former reveals that the redox activity of this Fe_8 system is confined within its cubane core. The resulting $(Fe_4O_4)^{3+}$-cubane, which is valence-delocalized in the NMR, Mössbauer, and IR spectroscopy time scales but valence-trapped in the X-ray photoelectron spectroscopy (XPS) time scale, is better described as a Robin−Day class-II system by the analysis of its near-infrared (NIR) intervalence charge transfer (IVCT) band profile.

Introduction

Intramolecular electron transfer processes associated with mixed-valence complexes are of fundamental importance in chemistry and physics, as well as in biology.[1] In-depth pioneering work on *dinuclear* charge transfer complexes by Taube, followed by seminal contributions by others, has established the theoretical basis for understanding these complexes and associated electron transfer events.[2] In contrast, the paucity of spectroscopic data on electron transfer phenomena pertaining to *polynuclear* transition metal complexes, as recently pointed out also by Keene and coworkers,[3] remains a challenge. The Fe−S proteins found in Nature containing redox active Fe_4S_4 cubanes are essential components in biological electron transfer processes, for example, photosynthesis, cell respiration, and nitrogen fixation, and as catalytic sites in hydrogenases.[4] While no analogous Fe_4O_4 cubane has been unequivocally characterized in a metalloprotein, the possibility of such a future discovery has been suggested.[5−7]

Earlier, the syntheses of a series of neutral all-Fe^{III} complexes, $[Fe_8(\mu_4\text{-}O)_4(4\text{-}R\text{-}pz)_{12}X_4]$, where pz = pyrazolato anion and X = Cl, R = H (**1**), Cl (**2**), or Me (**3**) and X= Br, R = H (**4**), were reported by us, along with the full spectroscopic, theoretical and magnetic study of **1**.[5] These complexes can be electrochemically reduced in four consecutive steps from the homovalent $[Fe_8]$ to the mixed valent $[Fe_8]^{4-}$.[5] The octanuclear complexes **1**−**4** contain two types of Fe^{III} sites, six-coordinate cubane-Fe (Fe_c) and five-coordinate outer-Fe (Fe_o), either one or both of which can be the site of redox activity (Scheme 1). The present work focuses on the structural and spectroscopic characterization of the $[Fe_8]^-$ species $\mathbf{2}^-$ in an effort to identify the site of redox activity and probe the issue of charge localization/delocalization in the mixed valence complex. Two more Fe^{III} complexes containing $Fe_8(\mu_4\text{-}O)_4$ cores similar to those of

* To whom correspondence should be addressed. E-mail: Raphael@adam.uprr.pr.
† University of Puerto Rico.
‡ Present address: Department of Chemistry, Juniata College, Huntingdon, Pennsylvania 16652.
§ NCSR "Demokritos".

(1) Bersuker, I. B.; Borshch, S. A. *Adv. Chem. Phys.* **1992**, *81*, 703.
(2) (a) Tom, G. M.; Creutz, C.; Taube, H. *J. Am. Chem. Soc.* **1974**, *96*, 7827. (b) Allen, C. G.; Hush, N. S. *Prog. Inorg. Chem.* **1967**, *8*, 357. (c) Creutz, C. *Prog. Inorg. Chem.* **1983**, *30*, 1. (d) Demadis, K. D.; Hartshorn, C. M.; Meyer, T. J. *Chem. Rev.* **2001**, *101*, 2655. (e) Day, P.; Hush, N. S.; Clark, R. J. H. *Philos. Trans. R. Soc. A* **2008**, *366*, 5.
(3) D'Allessandro, D. M.; Keene, R. R. *Chem. Rev.* **2006**, *106*, 2270.
(4) Rao, P. V.; Holm, R. H. *Chem. Rev.* **2004**, *104*, 527.
(5) (a) Baran, P.; Boca, R.; Chakraborty, I.; Giapintzakis, J.; Herchel, R.; Huang, Q.; McGrady, J. E.; Raptis, R. G.; Sanakis, Y.; Simopoulos, A. *Inorg. Chem.* **2008**, *47*, 645. (b) Raptis, R. G.; Georgakaki, I. P.; Hockless, D. C. R. *Angew.Chem., Int. Ed.* **1999**, *38*, 1632.
(6) Lee, D.; Sorace, L.; Caneschi, A.; Lippard, S. J. *Inorg. Chem.* **2001**, *40*, 6774.
(7) Fank, P.; De Tomaso, A.; Hedman, B.; Hodgson, K. O. *Inorg. Chem.* **2006**, *45*, 3920.

10.1021/ic801459s CCC: $40.75
Published on Web 11/08/2008

Scheme 1

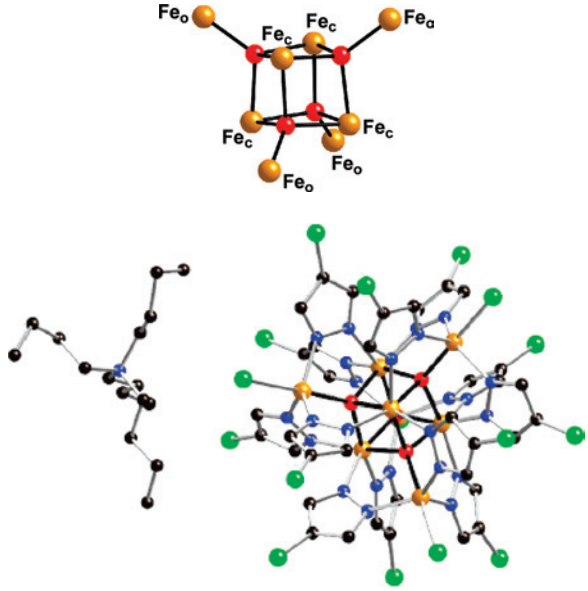

Figure 1. X-ray crystal structure of [^{n}Bu$_4$N$^+$][**2**$^-$]: Fe, gold; O, red; N, blue; Cl, green.

Table 1. Selected Bond Distances (Å) and Interatomic Angles (deg) for **2** and **2**$^-$

	2[a]	**2**$^-$
Fe$_c$−O	2.047(2)	2.039(2)−2.050(2)
Fe$_c$−N	2.101(3)	2.086(3)−2.103(3)
Fe$_c$···Fe$_c$	3.073(2)	3.061(2)−3.064(2)
Fe$_c$−O−Fe$_c$	97.3(2)	96.05(10)−97.32(10)
O−Fe$_c$−O	82.2(2)	82.19(9)−83.43(10)
Fe$_o$−O	1.930(4)	1.919(2), 1.931(2)
Fe$_o$−Cl	2.293(2)	2.279(1), 2.299(1)
Fe$_o$−N	2.028(3)	2.012(3)−2.043(3)
O−Fe$_o$−Cl	180.0(1)	178.71(9), 178.73(8)
N−Fe$_o$−N	119.6(1)	118.45(13)−120.81(14)
Fe$_o$···Fe$_o$	5.843(2)	5.849(2)−5.885(2)
Fe$_o$···Fe$_c$[b]	3.4432(8)	3.441(2), 3.448(2)
Fe$_o$···Fe$_c$[b]	5.460(1)	5.450(2)−5.457(2)

[a] Reference 5a. [b] There are three short and one long Fe$_o$···Fe$_c$ distances per Fe atom, between the vertexes of cocentrical tetrahedra formed by the four Fe$_c$ and four Fe$_o$ atoms, respectively.

1−**4** are known, but their redox activity has not been reported.[8,9]

Results and Discussion

The reaction of **2** with 1 equiv. of ^{n}Bu$_4$NBH$_4$ in CH_2Cl_2 yields the corresponding monoanion **2**$^-$, isolated in crystalline form as [^{n}Bu$_4$N$^+$][**2**$^-$] after slow evaporation of the mother liquor.[7] The X-ray crystal structure of [^{n}Bu$_4$N$^+$][**2**$^-$] is shown in Figure 1. Anionic **2**$^-$ crystallizes in an orthorhombic lattice with a crystallographic 2-fold axis running through the centers of two opposite (Fe$_c$)$_2$O$_2$ cubane faces and one-half anion per asymmetric unit. The overall symmetry of **2** (*T* point group) is preserved in the structure of **2**$^-$ with only statistically insignificant differences between corresponding bond lengths and angles (Table 1).[5a] This observation is consistent with charge delocalization within the Fe$_8$O$_4$ core.

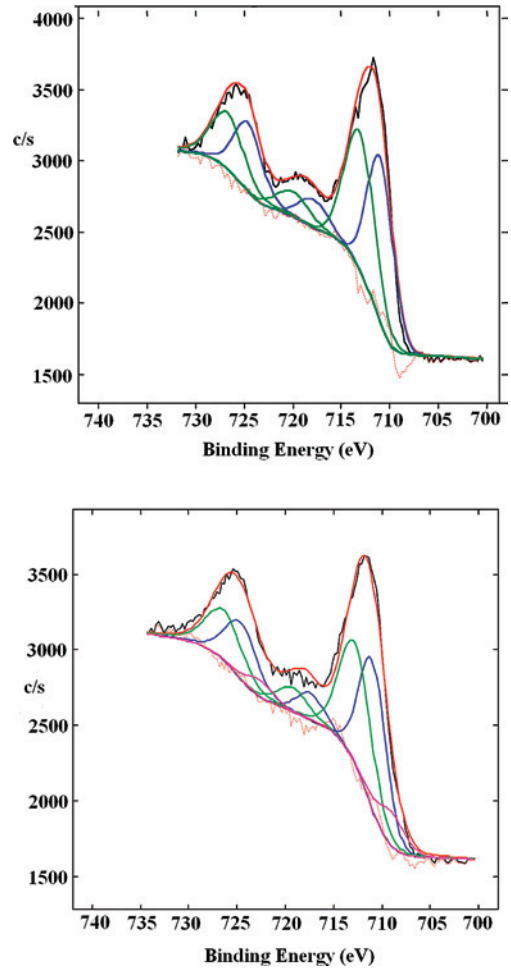

Figure 2. XPS spectra in the Fe-2p region of **2** (top) and [^{n}Bu$_4$N$^+$][**2**$^-$] (bottom): outer-Fe^{III}, blue trace; cubane-Fe^{III}, green trace; cubane-Fe^{II}, pink trace. The feature at 719 eV is a satellite of the main 2p$_{3/2}$ peak.

Crystallographic disorder could mask charge localization, although this interpretation is inconsistent with the spectroscopic evidence presented here (*vide infra*).

The solution ^{1}H NMR spectrum of **2**$^-$ reveals only one set of paramagnetically shifted resonances for the pyrazole H atoms, suggesting magnetic equivalence of all 12 pyrazolate rings. The most notable feature of the solid-state IR spectrum is the occurrence of a single ν(Fe−O) stretch, observed at 487 cm^{-1} for [^{n}Bu$_4$N$^+$][**2**$^-$], representing a 12 cm^{-1} shift to higher energy compared with that of **2**.[5a] Both NMR and IR results are consistent with charge delocalization at the respective time scales.

The Fe-2p XPS spectra of solid **2** and [^{n}Bu$_4$N$^+$][**2**$^-$] are shown in Figure 2. For **2**, deconvolution of the Fe-2p$_{3/2}$ and Fe-2p$_{1/2}$ peaks, each into two components, identifies the equal contributions of the five-coordinate outer-Fe^{III} atoms (711 and 725 eV) and six-coordinate cubane-Fe^{III} atoms (713 and 727 eV). Significantly, the deconvolution of the spectrum of [^{n}Bu$_4$N$^+$][**2**$^-$] requires the inclusion of the above two Fe^{III} components, now with unequal contributions, as well as that of a third component at 709 and 723 eV, the latter assigned to a cubane-Fe^{II} center. The decrease of intensity of only one of the two sets of XPS peaks indicates that the one-electron reduction is limited to one of the two sites. Mössbauer spectroscopy (*vide infra*) identifies the Fe$_4$O$_4$

(8) Hahn, F. E.; Jocher, C.; Lügger, T. *Z. Naturforsch.* **2004**, *59b*, 855.
(9) Gass, I. A.; Milios, C. J.; Whittaker, A. G.; Fabiani, F. P. A.; Parsons, S.; Murrie, M.; Perlepes, S. P.; Brechin, E. K. *Inorg. Chem.* **2006**, *45*, 5281.

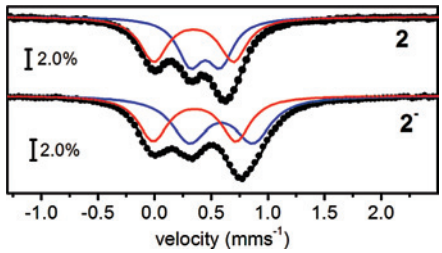

Figure 3. ^{57}Fe Mössbauer spectra of powder samples of **2** and [^{n}Bu$_4$N$^+$][**2**$^-$] at 78 K. Solid lines are simulations assuming two nested doublets for **2** and two crossed doublets for **2**$^-$. Blue = cubane-Fe; red = outer-Fe.

Table 2. ^{57}Fe Mössbauer Parameters of **2** and [^{n}Bu$_4$N$^+$][**2**$^-$] at 78 K

Fe site	δ (mm/s)	ΔE_Q (mm/s)
	2	
cubane	0.45(1)	0.26(2)
outer	0.34(1)	0.70(2)
	[^{n}Bu$_4$N$^+$][**2**$^-$]	
cubane	0.59(1)	0.56(2)
outer	0.35(1)	0.73(2)

cubane as the reduction site. The identification of distinct cubane-Fe^{III} and cubane-Fe^{II} sites in **2**$^-$ indicates charge localization at the XPS time scale (10^{-17} s).

The Mössbauer spectra of **2** and **2**$^-$ at 78 K (Figure 3) comprise three lines, the latter showing a characteristic shift of the highest energy line of ~0.14 mm s^{-1} toward higher values, indicative of an overall increase of both isomer shift (δ) and quadruple splitting (ΔE_Q) parameters, as expected for a one-electron reduction of **2**. Moreover, a doublet accounting for $^1/_8$ of total iron attributable to a high-spin Fe^{II} site is clearly absent in the spectrum of **2**$^-$, excluding the possibility that the one-electron reduction is localized on a specific iron site. Spectra of **2**$^-$ recorded in the 4.2−300 K range exhibit little variation (apart from a second-order Doppler effect-dependent shift), suggesting that delocalization persists over the entire temperature range at the Mössbauer time scale.

The simulation of **2** assumes two nested doublets in agreement with the earlier interpretation of the Mössbauer spectrum of **1**.[5a] Two crossed quadruple doublets are used for **2**$^-$, showing that the one-electron reduction leaves the outer Fe sites unaffected, while both δ and ΔE_Q increase substantially (Table 2). The average increase of 0.14 mm s^{-1} of the isomer shift of the four cubane-Fe sites upon one electron reduction is equivalent to an increase of 4 × 0.14 = 0.56 mm s^{-1} for a single Fe-atom, which is the expected increase for a high-spin Fe^{III} to a high-spin Fe^{II} transition.[10] An alternative simulation of the spectrum of **2**$^-$ using a two nested doublet model (Supporting Information) suggests delocalization over both types of Fe sites, inconsistent with the XPS spectroscopic results, which show that reduction is restricted to one of the two Fe sites.

A UV−vis−NIR spectrum was recorded for [^{n}Bu$_4$N$^+$][**2**$^-$] in CH_2Cl_2 solution at 298 K. In the UV−vis region, the LMCT band manifolds of **2** shift to lower energy in the spectrum of **2**$^-$ (Supporting Information). In the NIR region

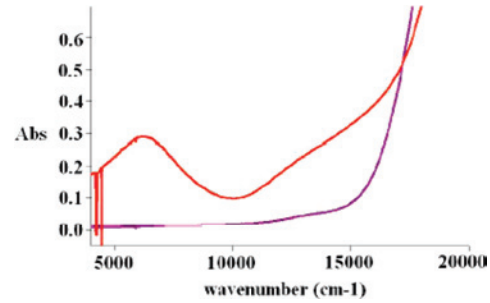

Figure 4. NIR spectra of **2** and **2**$^-$ (red) in CH_2Cl_2, 298 K.

Scheme 2

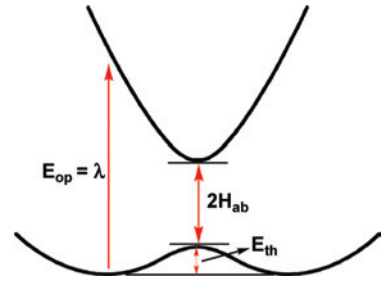

(Figure 4), a new weak band at ν_{max} = 6270 cm^{-1} (ε = 2500 dm^3 mol^{-1} cm^{-1}, $\Delta\nu_{1/2}$ = 3330 cm^{-1}) for **2**$^-$ was observed and assigned to an intervalence charge transfer (IVCT) transition, excluding the possibility of a valence-trapped situation (*localization*).[2b] The spectrum of **2**$^-$ was also recorded in CH_3CN, THF, and $(CH_3)_2CO$ with no observable effect on position and intensity of the IVCT band. The occurrence of the IVCT band in an otherwise clear region of the spectrum allows its analysis on the basis of classical two-state theory.[2b] The theoretical foundation for such analyses has been based on studies of dinuclear Creutz−Taube type systems but is equally applicable to polynuclear ones.[3] The experimental bandwidth at half-height, $\Delta\nu_{1/2}$, is narrower than the corresponding theoretical one, $\Delta\nu^0_{1/2}$, given by $\Delta\nu^0_{1/2}/\text{cm}^{-1} = [16RT\ln(2)\,\nu_{max}]^{1/2} = 3777$ cm^{-1}, where $16RT\ln(2) = 2310$ cm^{-1} at 298 K. Subsequently, the empirical parameter $\Gamma = 1 - (\Delta\nu_{1/2})/(\Delta\nu^0_{1/2})$ takes the value $\Gamma = 0.12$, classifying this species as a Robin−Day type-II system ($0 < \Gamma < 0.5$), or a weakly coupled delocalized system. The electronic coupling factor H_{ab} is estimated by $H_{ab} = 2.06 \times 10^{-2}(\nu_{max}\ \varepsilon_{max}\ \Delta\nu_{1/2})^{1/2}/r_{ab}$, taking the value H_{ab} = 1540 cm^{-1}.[11] The above value, calculated here using the average of the crystallographically determined Fe−Fe distances within the mixed-valent Fe_4O_4 cubane, r_{ab} = 3.061 Å, represents only the lower H_{ab} limit.[2d]

Scheme 2 shows a potential energy versus nuclear configuration plot for a Robin−Day type-II system, like **2**$^-$. The energy of optical electron transfer, E_{op}, is equal to the reorganization energy, λ = 6270 cm^{-1} for **2**$^-$. The reorganization energy is further analyzed into inner (λ_i, internal structural reorganization) and outer (λ_o, solvent reorganization) components, $\lambda = \lambda_i + \lambda_o$. Because of the solvent-independent behavior of the IVCT band of **2**$^-$, we estimate

(10) Parish, R. V. *NMR, NQR, EPR and Mössbauer Spectroscopy in Inorganic Chemistry*, Ellis Horwood Ltd.: Chichester, U.K., 1990.

(11) (a) Robin, M. B.; Day, P. *Adv. Inorg. Chem. Radiochem.* **1967**, *10*, 247. (b) Brunschwig, B. S.; Creutz, C.; Sutin, N. *Chem. Soc. Rev.* **2002**, *31*, 168.

that λ_o is a minor contributor to λ and $\lambda_i \leq 6000$ cm^{-1}. E_{th} is the thermal energy barrier between the degenerate states. Because the electronic coupling, H_{ab}, is smaller than $\lambda/2$, the lower surface energy consists of double minima. For such systems, the thermal electron transfer barrier, E_{th}, is given by $E_{th} = (\lambda/4) - H_{ab}$, taking the value of $E_{th} = 28$ cm^{-1} for $\mathbf{2}^-$.[2c]

In summary, the spectroscopic data presented here confine the value of electron-transfer rate among the Fe centers of the mixed valent Fe_4O_4-cubane of $\mathbf{2}^-$ between the time scale limits of those probes that identify the charge as delocalized, (X-ray crystallography, ^{1}H NMR (seconds), and Mössbauer and IR spectroscopy (10^{-8} s, slow limit)), and the time scale of XPS (10^{-17} s, fast limit), which identifies it as localized. The time scale of electronic spectroscopy ($\sim 10^{-15}$ s), which classifies $\mathbf{2}^-$ as a weakly coupled system, is our current best estimate of the electron-transfer rate. Examples of other delocalized systems exhibiting valence localization of the ground state at the XPS time scale exist in the literature.[12] The present study provides an entry to the spectroscopic investigation of oxo-analogues of the well-studied and biologically relevant Fe_4S_4-cubanes.[4] The spectroscopic data of $(Fe_4O_4)^{4+}$ and $(Fe_4O_4)^{3+}$ may assist the recognition of the Fe_4O_4-cubane motif in an electron-transfer protein, if such proteins indeed exist.[5,7] Detailed spectroscopic, magnetic, kinetic and theoretical studies of the above species, as well as of their corresponding $(Fe_4O_4)^{2+/+/0}$ redox-modified derivatives, are currently in progress.

Experimental Section

$FeCl_3$, pyrazole, and tetrabutyl ammonium borohydride (^{n}Bu$_4$NBH$_4$) were obtained from commercial sources and used as received. 4-Cl-pyrazole was prepared by a literature procedure.[13] Anhydrous CH_2Cl_2 (99.8%) was obtained from commercial source and any other solvent was taken from MBraun solvent purification system.

Synthesis of [^{n}Bu$_4$N$^+$][2$^-$]. ^{n}Bu$_4$NBH$_4$ (7.7 mg, 0.030 mmol) was added to a CH_2Cl_2 (anhydrous, 15 mL) solution of **2** (50 mg, 0.027 mmol) under N_2, resulting in an immediate color change from reddish orange to yellowish brown. The solution was stirred for 2 h and filtered, and the filtrate was taken to dryness under reduced pressure to obtain a brown solid, which was dried under vacuum over $CaCl_2$ overnight. The dry solid was washed with anhydrous MeOH and stored under N_2. X-ray quality crystals (Yield: 47 mg, 84%) were grown by slow evaporation of a [^{n}Bu$_4$N$^+$][**2**$^-$]/CH_2Cl_2 solution. ^{1}H NMR ($CDCl_3$, ppm): 14.93 (H^3, s, $w_{1/2} = 102$ Hz), 7.65 (H^5, s, $w_{1/2} = 66$ Hz), 108−3.15 (^{n}Bu). UV−vis−NIR (CH_2Cl_2, cm^{-1}): 28 330 ($\varepsilon = 80\,000$ mol^{-1} cm^{-1}), 22 000 (shoulder), 6270 ($\varepsilon = 2500$ dm^3 mol^{-1} cm^{-1}). IR (KBr pellet, cm^{-1}): 486 (s), 571 (vw), 614 (w), 2760 (m), 959 (w), 1043 (s), 1143 (w), 1170 (m), 1268 (s), 1365 (s), 1417 (m), 1490 (m), 2871 (w), 2932 (w), 2961 (w).

Table 3. Crystallographic Data for [^{n}Bu$_4$N$^+$][**2**$^-$]

formula	$C_{52}H_{60}N_{25}Cl_{16}O_4Fe_8$
crystal size, mm^3	0.15 × 0.14 × 0.07
fw	2113.25
space group	*Pbcn*
a, Å	18.078(4)
b, Å	26.212(5)
c, Å	18.023(4)
V, Å^3	8540(3)
Z	4
ρ_{calcd}, Mg m^{-3}	1.644
$2\theta_{max}$, deg	56.54
μ(Mo Kα), mm^{-1}	1.875
reflns collected	53521
unique reflns, $I > 2\sigma(I)$	9905/4353
no. of params/restraints	476/5
R_1[a]/GOF[b]	0.0399/0.863
wR_2[c] ($I > 2\sigma(I)$)	0.0883

[a] $I > 2\sigma(I)$; $R_1 = \sum||F_o| - |F_c||/\sum|F_o|$. [b] GOF = $[\sum[w(F_o^2 - F_c^2)^2]/(n - p)]^{1/2}$. [c] $wR_2 = [\sum[w(F_o^2 - F_c^2)^2/\sum[w(F_o^2)^2]]^{1/2}$, where $w = 1/\sigma^2(F_o^2) + (aP)^2 + bP$, $P = (F_o^2 + 2F_c^2)/3$.

Physical Measurements. The electronic spectra of the complexes in solution were recorded on a Varian CARY 500 scan instrument in 200−3200 nm range. Infrared spectra (KBr pellets) were recorded on Nicolet 750 FTIR spectrophotometer. ^{1}H NMR data were recorded on a Bruker AVANCE DPX-300 spectrometer. Mössbauer spectra were recorded with powdered samples with a constant acceleration conventional spectrometer with a source of ^{57}Co (Rh matrix). Spectra in the 4.2−300 K temperature range were obtained using an Oxford cryostat. Isomer shift values (δ) are reported relative to iron foil at 293 K. XPS measurements were carried out with a PHI 5600 ESCA system (Physical Electronics). The spectra were analyzed by using the program *WMOSS* (Web Research, Edina, MN).

X-ray Crystallographic Data Collection and Refinement of the Structure. X-ray diffraction data for [^{n}Bu$_4$N$^+$][**2**$^-$] was collected from a single crystal mounted atop a glass fiber with a Siemens SMART 1K CCD diffractometer[14a] and was corrected for Lorentz and polarization effects.[14b] The structure was solved employing the *SHELX-90*[14c] program and refined by least-squares methods on F^2 via *SHELXTL-93*,[14d] incorporated in *SHELXTL*, version 5.1.[14e] Crystallographic details for [^{n}Bu$_4$N$^+$][**2**$^-$] are summarized in Table 3.

Acknowledgment. Financial support from NIH SCoRE S06GM008102 is acknowledged.

Supporting Information Available: Spectroscopic data and crystallographic information file for [^{n}Bu$_4$N$^+$][**2**$^-$]. This material is available free of charge via the Internet at http://pubs.acs.org.

IC801459S

(12) Citrin, P. H.; Ginsberg, A. P. *J. Am. Chem. Soc.* **1981**, *103*, 3673.
(13) Ehlert, M. K.; Rettig, S. J.; Storr, A.; Thompson, R. C.; Trotter, J. *Can. J. Chem.* **1991**, *69*, 432.
(14) (a) *SMART-NT Software Reference Manual*, version 5.059; Bruker AXS, Inc.: Madison, WI, 1998. (b) *SAINT+ Software Reference Manual*, version 6.02; Bruker AXS, Inc.: Madison, WI, 1999. (c) Sheldrick, G. M. *SHELXS-90, Program for Solution of Crystal Structure*; University of Gottingen: Gottingen, Germany, 1986. (d) Sheldrick, G. M. *SHELXL-97, Program for Refinement of Crystal Structure*; University of Gottingen: Gottingen, Germany, 1997. (e) *SHELXTL-NT Software Reference Manual*, version 5.1; Bruker AXS, Inc.: Madison, WI, 1998.